

---

# Preferred-Action-Optimized Diffusion Policies for Offline Reinforcement Learning

---

Tianle Zhang<sup>1</sup>, Jiayi Guan<sup>1,2</sup>, Lin Zhao<sup>1,3</sup>, Yihang Li<sup>1</sup>, Dongjiang Li<sup>1</sup>, Zecui Zeng<sup>1</sup>, Lei Sun<sup>1</sup>, Yue Chen<sup>1</sup>, Xuelong Wei<sup>1</sup>, Lusong Li<sup>1</sup>, Xiaodong He<sup>1</sup>

<sup>1</sup>JD Explore Academy, China

<sup>2</sup>Tongji University, China

<sup>3</sup>Beijing Institute of Technology, China

tianle-zhang@outlook.com, guanjiayi@tongji.edu.cn, zhaolins@foxmail.com, {liyihang18, lidongjiang5, zengzecui1}@jd.com, {sunlei155, chenye21, weixuelong1}@jd.com, lilusong@gmail.com, xiaodong.he@jd.com

## Abstract

Offline reinforcement learning (RL) aims to learn optimal policies from previously collected datasets. Recently, due to their powerful representational capabilities, diffusion models have shown significant potential as policy models for offline RL issues. However, previous offline RL algorithms based on diffusion policies generally adopt weighted regression to improve the policy. This approach optimizes the policy only using the collected actions and is sensitive to Q-values, which limits the potential for further performance enhancement. To this end, we propose a novel preferred-action-optimized diffusion policy for offline RL. In particular, an expressive conditional diffusion model is utilized to represent the diverse distribution of a behavior policy. Meanwhile, based on the diffusion model, preferred actions within the same behavior distribution are automatically generated through the critic function. Moreover, an anti-noise preference optimization is designed to achieve policy improvement by using the preferred actions, which can adapt to noise-preferred actions for stable training. Extensive experiments demonstrate that the proposed method provides competitive or superior performance compared to previous state-of-the-art offline RL methods, particularly in sparse reward tasks such as Kitchen and AntMaze. Additionally, we empirically prove the effectiveness of anti-noise preference optimization.

## 1 Introduction

Offline reinforcement learning (RL) seeks to learn effective policies from previous experiences without interacting with the environment [1]. Avoiding costly or risky online interactions makes offline RL appealing for numerous real-world applications. Extending online RL methods to the offline setting primarily faces the issue of distribution shift [2]. Existing offline RL methods predominantly concentrate on addressing this issue by employing conservative updates for Q-functions [3–5], constraining a policy to stay close to the behavior policy via weighted regression (WR) [6, 7], or integrating the two approaches [8, 9]. However, most offline RL methods usually parameterize a policy as an unimodal Gaussian model with the learned mean and variance. This scheme may not be feasible when the collected data distribution is complex and diverse. Moreover, the collected behaviors can be highly diverse in the real world and present strong multi-modalities [10]. Therefore, more expressive policy models are urgently needed.

Fortunately, diffusion models [11, 12] are usually used to model diverse or multimodal distributions due to their strong expressiveness, and have achieved the latest benchmark in image generation tasks [13, 14]. Recently, the offline RL works using the diffusion model as a policy model have shown great potential [15] and made good progress [10]. Despite the impressive improvement that these works have achieved, they still adopt the WR method [6] for policy improvement. However, the WR method has two critical drawbacks preventing the performance improvement of diffusion policies. *First*, WR aims to help prevent querying out-of-sample actions, which can result in policy performance being greatly limited by the collected data. In most offline tasks, the collected data is only a small part of the whole state-action space. Thus, WR has a performance upper constraint and cannot greatly improve the performance of policies. *Second*, WR typically uses Q-value to calculate the updated weights of policies and is sensitive to Q-value. In offline RL, the estimation of the Q-value generally exits error due to the out-of-distribution (OOD) problem [16]. Consequently, WR sensitive to Q-value has unstable training, which can degrade performance.

Recently, RL with preference-based reward learning has shown great potential for further improving the performance of large language models [17]. Meanwhile, direct preference optimization (DPO) [18] deduces that a simple classification loss using preference models can be directly used to solve the RL problem for policy improvement. Inspired by this, we propose a novel **Preferred-Action-Optimized Diffusion Policy** (PAO-DP) for offline RL. PAO-DP focuses on utilizing preferred actions to optimize the diffusion policy via a preference model (e.g., Bradley-Terry [19]), instead of WR. To our knowledge, PAO-DP is the first attempt to integrate preference optimization with diffusion models for offline RL. Specifically, PAO-DP mainly has the following characteristics: 1) The diverse distribution of the behavior policy is represented using a conditional diffusion model by the behavior cloning approach. 2) Preferred actions are automatically generated by the critic function based on the diffusion model, rather than manually annotating. All preferred actions are sampled from the same distribution of the behavior policy for accuracy evaluation. 3) An anti-noise preference optimization is designed to improve the diffusion policy further by using preferred actions, while also handling noise-preferred actions for stable training. We test PAO-DP on the popular D4RL benchmarking [20]. The experiment results demonstrate the proposed method achieves competitive or superior performance compared with prior offline RL methods, especially in sparse-reward tasks such as Kitchen and AntMaze.

## 2 Preliminaries

### 2.1 Offline Reinforcement Learning

**Offline RL Settings.** A decision-making problem is usually modeled as a Markov decision process (MDP). The MDP is defined as a tuple [21]:  $(\mathcal{S}, \mathcal{A}, \mathcal{P}, r, \gamma)$ , where  $\mathcal{S}$  and  $\mathcal{A}$  denote the state and action spaces respectively,  $\mathcal{P}(s'|s, a) : \mathcal{S} \times \mathcal{A} \times \mathcal{S} \rightarrow [0, 1]$  denotes the transition probability from state  $s$  to the next state  $s'$  after taking the action  $a$ ,  $r : \mathcal{S} \times \mathcal{A} \rightarrow \mathbb{R}$  represents the reward function,  $\gamma \in [0, 1)$  is the discount factor. The goal is to learn a policy  $\pi(a|s)$  that maximizes the cumulative discounted reward  $\sum_{t=0}^{\infty} \gamma^t r(s_t, a_t)$ . In an offline setting, the objective is to learn a policy that maximizes reward from a static sample dataset  $\mathcal{D}$  collected by an unknown behavioral policy  $\pi^b$ , without further online interaction with the environment [22, 23].

**Weighted Regression.** In offline RL algorithms, due to the importance of adhering to the behavior policy  $\pi^b$ , previous works [24, 6] explicitly constraint the learned policy  $\pi$  to be closed to  $\pi^b$ , while maximizing the expected value of the Q-function [25]:

$$J(\pi) = \arg \max_{\pi} \mathbb{E}_s \left[ \sum_a \pi(a|s) Q_{\phi}(s, a) \right] - \eta \mathbb{E}_s \left[ D_{KL}(\pi(\cdot|s) || \pi^b(\cdot|s)) \right]. \quad (1)$$

The first term corresponds to the optimization objective of the policy  $\pi$ , in which  $Q_{\phi}$  is a learned Q-function of  $\pi$ . The second term acts as a regularization term to constrain the learned policy within the bounds of the dataset  $\mathcal{D}$  with  $\eta$  being the coefficient. By solving the Eq. (1) for the extreme points of the policy  $\pi$ , the closed-form solution for the optimal policy  $\pi^*$  can be obtained [6]:

$$\pi^* = \frac{1}{Z(s)} \pi^b(a|s) \exp\left(\frac{1}{\eta} Q_{\phi}(s, a)\right), \quad (2)$$

where  $Z(s)$  is the partition function. Eq. (2) can be regarded as a policy improvement step. Due to the difficulty in modeling the behavior policy  $\pi^b$  and the problem of inaccurate estimation of the

Q-function, it is challenging to sample and obtain the optimal action directly. The existing methods [24, 8, 22, 25] typically project the optimal policy  $\pi^*$  onto a parameterized policy  $\pi_\theta$  to bypass this issue:

$$\arg \min_{\theta} \mathbb{E}_{\mathbf{s} \sim \mathcal{D}} [D_{KL}(\pi^*(\cdot|\mathbf{s})||\pi_\theta(\cdot|\mathbf{s}))] = \arg \max_{\theta} \mathbb{E}_{(\mathbf{s}, \mathbf{a}) \sim \mathcal{D}} \left[ \frac{1}{Z(\mathbf{s})} \log \pi_\theta(\mathbf{a}|\mathbf{s}) \exp\left(\frac{1}{\eta} Q_\phi(\mathbf{s}, \mathbf{a})\right) \right]. \quad (3)$$

Such a method is commonly known as weighted regression, where  $\exp(\frac{1}{\eta} Q_\phi(\mathbf{s}, \mathbf{a}))$  serves as the regression weights.

## 2.2 Diffusion Probabilistic Model

Diffusion-based generative models [26, 11] mainly include forward and reverse diffusion processes. In particular, suppose there is a real data distribution  $q(x)$ , from which a sample  $x^0 \sim q(x)$  is drawn. The forward diffusion process followed a Markov chain gradually adds Gaussian noise to the sample through  $K$  incremental steps, yielding a sequence of noisy samples  $x^1, \dots, x^K$  controlled by a pre-defined variance schedule  $\beta^1, \dots, \beta^K$ . The forward process is expressed as:

$$q(\mathbf{x}^{1:K}|\mathbf{x}^0) = \prod_{k=1}^K q(\mathbf{x}^k|\mathbf{x}^{k-1}), \quad q(\mathbf{x}^k|\mathbf{x}^{k-1}) = \mathcal{N}(\mathbf{x}^k; \sqrt{1 - \beta^k} \mathbf{x}^{k-1}, \beta^k \mathbf{I}). \quad (4)$$

In the reverse diffusion processes, diffusion models mainly learn a conditional distribution  $p_\theta(\mathbf{x}^{k-1}|\mathbf{x}^k)$  for generating new samples. The reverse process is represented as:

$$p_\theta(\mathbf{x}^{0:K}) = p(\mathbf{x}^K) \prod_{k=1}^K p_\theta(\mathbf{x}^{k-1}|\mathbf{x}^k), \quad p_\theta(\mathbf{x}^{k-1}|\mathbf{x}^k) = \mathcal{N}(\mathbf{x}^{k-1}; \boldsymbol{\mu}_\theta(\mathbf{x}^k, k), \boldsymbol{\Sigma}_\theta(\mathbf{x}^k, k)), \quad (5)$$

where  $p(\mathbf{x}^K) = \mathcal{N}(\mathbf{0}, \mathbf{I})$ . The diffusion training is executed by maximizing the evidence lower bound (ELBO):  $\mathbb{E}_q[\ln p_\theta(\mathbf{x}^{0:K}) - \ln q(\mathbf{x}^{1:K}|\mathbf{x}^0)]$  [27, 10].

## 3 Method

In this section, we detail the overall design of the proposed preferred-action optimized diffusion policy (PAO-DP). Firstly, we formulate an RL behavior policy using a conditional diffusion model. Then, the preferred-action automatic generation module is presented. The module aims to utilize the behavior policy and critic function to generate preferred actions. Finally, the policy anti-noise preference optimization is given to achieve policy improvement by using the preferred actions.

### 3.1 Conditional Diffusion Policy

Generally, the reverse process of a conditional diffusion model is used as an RL parametric policy [15, 10]:

$$\pi_\theta^b(\mathbf{a}_t|\mathbf{s}_t) = p_\theta(\mathbf{a}_t^{0:K}|\mathbf{s}_t) = p(\mathbf{a}_t^K) \prod_{k=1}^K p_\theta(\mathbf{a}_t^{k-1}|\mathbf{a}_t^k, \mathbf{s}_t), \quad (6)$$

where  $k \in \{1, \dots, K\}$  denotes the diffusion timestep,  $t \in \{1, \dots, T\}$  represents the trajectory timestep,  $\mathbf{a}^K \sim \mathcal{N}(\mathbf{0}, \mathbf{I})$ . Herein, the end sample  $\mathbf{a}^0$  of the reverse chain is the action for the RL policy.  $p_\theta(\mathbf{a}_t^{k-1}|\mathbf{a}_t^k, \mathbf{s}_t)$  can usually be modeled as a Gaussian distribution. Following the denoising diffusion probabilistic model (DDPM) [11],  $p_\theta(\mathbf{a}_t^{k-1}|\mathbf{a}_t^k, \mathbf{s}_t)$  is parameterized as a noise prediction model with a fixed covariance matrix:  $\boldsymbol{\Sigma}_\theta(\mathbf{a}_t^k, k; \mathbf{s}_t) = \eta^k \mathbf{I}$  and mean built as:

$$\boldsymbol{\mu}_\theta(\mathbf{a}_t^k, k; \mathbf{s}_t) = \frac{1}{\sqrt{\alpha_k}} \left( \mathbf{a}_t^k - \frac{\beta_k}{\sqrt{1 - \bar{\alpha}_k}} \boldsymbol{\epsilon}_\theta(\mathbf{a}_t^k, k; \mathbf{s}_t) \right), \quad (7)$$

where  $\alpha^k = 1 - \beta^k$ ,  $\bar{\alpha}^k = \prod_{i=1}^k \alpha^i$ ,  $\boldsymbol{\epsilon}_\theta$  is a parametric noise model. In DDPM, we can obtain an action through the following sampling process:

$$\mathbf{a}_t^{k-1} = \frac{\mathbf{a}_t^k}{\sqrt{\alpha^k}} - \frac{\beta^k}{\sqrt{\alpha(1 - \bar{\alpha}^k)}} \boldsymbol{\epsilon}(\mathbf{a}_t^k, k; \mathbf{s}_t) + \sqrt{\beta^k} \boldsymbol{\epsilon}, \quad \boldsymbol{\epsilon} \sim \mathcal{N}(0, \mathbf{I}), \quad \text{for } k = K, \dots, 1. \quad (8)$$

Similar to DDPM, the objective proposed by [11] can be simplified to train the  $\boldsymbol{\epsilon}$  model by:

$$\mathcal{L}_d(\theta) = \mathbb{E}_{k \sim \mathcal{U}, \boldsymbol{\epsilon} \sim \mathcal{N}(0, \mathbf{I}), (\mathbf{s}_t, \mathbf{a}_t^0) \sim \mathcal{D}} [\|\boldsymbol{\epsilon} - \boldsymbol{\epsilon}_\theta(\sqrt{\bar{\alpha}_k} \mathbf{a}_t^0 + \sqrt{1 - \bar{\alpha}_k} \boldsymbol{\epsilon}, k; \mathbf{s}_t)\|^2], \quad (9)$$

where  $\mathcal{U}$  is a uniform distribution over  $\{1, \dots, K\}$  and  $\mathcal{D}$  denotes the offline dataset collected by a behavior policy  $\pi^b$ . The diffusion loss  $\mathcal{L}_d(\theta)$  aims to learn the behavior policy through the conditional diffusion model with  $\epsilon_\theta$ , and it is just a loss of behavior cloning. Herein,  $\pi_{\epsilon_\theta}^b(\mathbf{a}_t|\mathbf{s}_t)$  is used to represent the learned diffusion behavior policy.

### 3.2 Preferred-Action Automatic Generation

Based on the learned behavior policy, we further use preference optimization to achieve policy improvement, instead of weighted regression. One of the keys to preference optimization is to obtain preferred actions. In the field of preference learning [28], preference data is generally provided in advance. However, this requires a lot of manpower and material resources. To avoid this issue, we design an automatic acquisition approach that relies on the Q-function. Specifically, we need to automatically generate preferred-action samples, i.e.,  $\{\mathbf{s}_t, \mathbf{a}_t, \hat{\mathbf{a}}_t, \Gamma_{Q(\mathbf{s}_t, \mathbf{a}_t) > Q(\mathbf{s}_t, \hat{\mathbf{a}}_t)}\} \in \mathcal{D}_p$ , where  $\mathbf{a}_t$  denotes the behavior action corresponding to the state  $\mathbf{s}_t$  in the offline data  $\mathcal{D}$ ,  $\hat{\mathbf{a}}_t$  is another action obtained through the following sampling method,  $\Gamma_{Q(\mathbf{s}_t, \mathbf{a}_t) > Q(\mathbf{s}_t, \hat{\mathbf{a}}_t)}$  is a symbolic function used to determine which action has a larger Q-value:

$$\Gamma_{Q(\mathbf{s}_t, \mathbf{a}_t) > Q(\mathbf{s}_t, \hat{\mathbf{a}}_t)} = \begin{cases} 1, & Q(\mathbf{s}_t, \mathbf{a}_t) > Q(\mathbf{s}_t, \hat{\mathbf{a}}_t) \\ -1, & \text{otherwise} \end{cases}. \quad (10)$$

Meanwhile, the Q-function  $Q_\phi(\mathbf{s}_t, \mathbf{a}_t)$  parameterized by  $\phi$  can be learned by utilizing the existing Q-learning framework, e.g., TD3 [29] and implicit Q-learning (IQL) [5]

**Preferred-Action Sampling.** Considering the OOD problem in Q-value estimation, we hope another action  $\hat{\mathbf{a}}_t$  can be obtained from the distribution of the behavior policy. Due to the learned policy  $\pi_{\epsilon_\theta}^b$  modeling the distribution of the behavior policy,  $\hat{\mathbf{a}}_t$  can be sampled from  $\pi_{\epsilon_\theta}^b(\hat{\mathbf{a}}_t|\mathbf{s}_t)$  directly. Generally, higher-quality actions are beneficial for the improvement of policies, especially in preference learning. This further motivates us to sample the action  $\hat{\mathbf{a}}_t$  from the optimal policy  $\pi^*$ .

Since the exact and derivable density function of  $\pi^*$  cannot be determined, it is difficult to directly draw samples from  $\pi^*$ . Drawing on insights from [25] and according to Eq. (2), the optimal policy  $\pi^*$  can be further expressed as:

$$\pi^*(\mathbf{a}_t|\mathbf{s}_t) \propto \pi_{\epsilon_\theta}^b(\mathbf{a}_t|\mathbf{s}_t) \exp(\eta Q_\phi(\mathbf{s}_t, \mathbf{a}_t)), \quad (11)$$

Based on this formula, we use an importance sampling technique to sample actions. In particular, for each state  $\mathbf{s}_t$ , we firstly draw  $N$  actions from the learned behavior policy  $\pi_{\epsilon_\theta}^b$ . Then, these actions are evaluated with the learned Q-function  $Q_\phi$ . Finally, an action is drawn from  $N$  actions with  $\exp(\eta Q_\phi(\hat{\mathbf{a}}_t, \mathbf{s}_t))$  being the sampling weights [25]. Additionally, we can use greedy sampling to obtain  $\hat{\mathbf{a}}_t$  from  $N$  actions.

### 3.3 Policy Anti-Noise Preference Optimization

After obtaining the preferred action samples, the behavior policy  $\pi_{\epsilon_\theta}^b$  can be further improved stably by anti-noise preference optimization. Specifically, firstly, according to Eq. (2), we can obtain an expression for Q-function:

$$Q_\phi(\mathbf{s}_t, \mathbf{a}_t) = \eta \log \frac{\pi^*(\mathbf{a}_t|\mathbf{s}_t)}{\pi_{\epsilon_\theta}^b(\mathbf{a}_t|\mathbf{s}_t)} + \eta \log Z(\mathbf{s}_t). \quad (12)$$

Then, based on  $\{\mathbf{s}_t, \mathbf{a}_t, \hat{\mathbf{a}}_t, \Gamma_{Q(\mathbf{s}_t, \mathbf{a}_t) > Q(\mathbf{s}_t, \hat{\mathbf{a}}_t)}\}$ , the popular Bradley-Terry (BT) [19, 18] model is used to model the action preference distribution  $p^*$ :

$$p^*(\hat{\mathbf{a}}_t \succ \mathbf{a}_t|\mathbf{s}_t) = \frac{\exp(Q_\phi(\mathbf{s}_t, \hat{\mathbf{a}}_t))}{\exp(Q_\phi(\mathbf{s}_t, \hat{\mathbf{a}}_t)) + \exp(Q_\phi(\mathbf{s}_t, \mathbf{a}_t))}. \quad (13)$$

Putting the expression of Q in Eq. (12) into Eq. (13), we can obtain the action preference probability in terms of only the optimal policy  $\pi^*$  and the behavior policy  $\pi_{\epsilon_\theta}^b$ , expressed as [18]:

$$p^*(\hat{\mathbf{a}}_t \succ \mathbf{a}_t|\mathbf{s}_t) = \frac{1}{1 + \exp\left(\eta \log \frac{\pi^*(\mathbf{a}_t|\mathbf{s}_t)}{\pi_{\epsilon_\theta}^b(\mathbf{a}_t|\mathbf{s}_t)} - \eta \log \frac{\pi^*(\hat{\mathbf{a}}_t|\mathbf{s}_t)}{\pi_{\epsilon_\theta}^b(\hat{\mathbf{a}}_t|\mathbf{s}_t)}\right)}. \quad (14)$$

The derivation is in the Appendix B.2. Herein, we parameterize the optimal policy by  $\psi$ , represented as the surrogate optimal policy  $\pi_\psi$ , where the structure of  $\pi_\psi$  is the same as  $\pi_{\epsilon_\theta}^b$ , and  $\pi_\psi$  is further

optimized based on  $\pi_{\epsilon_\theta}^b$  for the policy improvement. Subsequently, we can formulate a maximum likelihood objective for  $\pi_\psi$ . The policy improvement objective can be expressed as:

$$\mathcal{L}_{imp}(\psi; \theta) = -\mathbb{E}_{(\mathbf{s}_t, \mathbf{a}_t, \hat{\mathbf{a}}_t, \Gamma) \in \mathcal{D}_p} \left[ \log \sigma \left( (\eta * \Gamma) \log \frac{\pi_\psi(\hat{\mathbf{a}}_t | \mathbf{s}_t)}{\pi_{\epsilon_\theta}^b(\hat{\mathbf{a}}_t | \mathbf{s}_t)} - (\eta * \Gamma) \log \frac{\pi_\psi(\mathbf{a}_t | \mathbf{s}_t)}{\pi_{\epsilon_\theta}^b(\mathbf{a}_t | \mathbf{s}_t)} \right) \right], \quad (15)$$

where  $\sigma$  is the logistic function. Furthermore, considering the imprecision possibility of estimating Q-values in offline RL, such inaccuracies may introduce noises in the preference action samples. This may lead to instability in training during the policy improvement process. To alleviate this issue, we further establish an anti-noise optimization objective. Specifically, assume that the preferred action label may be flipped with a small probability  $\lambda \in (0, 0.5)$  and  $\hat{\mathbf{a}}_t$  is preferred  $\mathbf{a}_t$ , we can obtain a conservative preferred-action probability  $p^*(\hat{\mathbf{a}}_t \succ \mathbf{a}_t | \mathbf{s}_t) = 1 - \lambda$  [30]. Hence, we can calculate a cross-entropy loss as the anti-noise optimization objective [31]:

$$\mathcal{L}_{anti}(\psi; \theta) = (1 - \lambda) \mathcal{L}_{imp}(\psi; \theta) + \lambda \mathcal{L}_{imp}^{-\Gamma}(\psi; \theta), \quad (16)$$

where  $\mathcal{L}_{imp}^{-\Gamma}(\psi; \theta)$  represents the objective whose preference actions have been flipped.

In our paper, to train more efficiently, we adopt a strategy of simultaneously training behavior policy  $\pi_{\epsilon_\theta}^b$  and surrogate optimal policy  $\pi_\psi$ , rather than dividing the training into two stages. Hence, the loss function of the surrogate optimal policy is a linear combination of policy cloning and policy improvement, represented as  $\mathcal{L}(\psi) = \mathcal{L}_d(\psi) + \xi \mathcal{L}_{anti}(\psi; \theta)$ , where  $\xi$  is a hyperparameter to provide a weight for the policy improvement part. This parameter can also be used to measure the effect of the policy improvement. The overall algorithm is given in Algorithm 1

---

#### Algorithm 1: PAO-DP Algorithm

---

**Input:** Dataset  $\mathcal{D} = \{(\mathbf{s}_t, \mathbf{a}_t, r_t, \mathbf{s}_{t+1})_{i=0}^n\}$

**Output:** Surrogate optimal policy  $\pi_\psi$ , Behavior policy  $\pi_{\epsilon_\theta}^b$

```

1 for each batch do
2   Sample a batch of transitions  $(\mathbf{s}_t, \mathbf{a}_t, r_t, \mathbf{s}_{t+1})$  from the buffer  $\mathcal{D}$ 
3   # Behavior policy learning
4   Update  $\epsilon_\theta$  via the Eq. (9)
5   # Critic learning
6   Update  $Q_\phi$  via the existing Q-learning method, e.g., IQL
7   # Preferred-action automatic generation
8   Sample  $N$  actions in  $\mathbf{s}_t$  by the behavior policy  $\pi_{\epsilon_\theta}^b$  using the Eq. (8)
9   Select an action from  $N$  actions via the importance sampling using Eq. (11)
10  Generate preferred-action sample  $\{\mathbf{s}_t, \mathbf{a}_t, \hat{\mathbf{a}}_t, \Gamma_{Q(\mathbf{s}_t, \mathbf{a}_t) > Q(\mathbf{s}_t, \hat{\mathbf{a}}_t)}\}$  via Eq. (10)
11  # Policy improvement
12  Calculate the anti-noise preference loss  $\mathcal{L}_{anti}(\psi; \theta)$  via Eq. (16)
13  Calculate the diffusion loss  $\mathcal{L}_d(\psi)$  via Eq. (9)
14  Update the surrogate optimal policy  $\pi_\psi$  via the total loss function:
     $\mathcal{L}(\psi) = \mathcal{L}_d(\psi) + \xi \mathcal{L}_{anti}(\psi; \theta)$ 

```

---

## 4 Experiments

We conduct extensive experiments on the popular D4RL benchmark [20] to validate the effectiveness of the proposed method, especially in sparse-reward tasks. Additionally, we performed ablation studies to dissect the contributions of the main components of PAO-DP. Furthermore, we carried out a parameter sensitivity analysis across different methods to assess their robustness and performance.

### 4.1 Experimental Settings

**Baselines.** The proposed method is evaluated in four different domains in D4RL, including Kitchen, AntMaze, Adroit, and Gym-locomotion. In our experiments, Kitchen and AntMaze are all composed of sparse-reward tasks, while Adroit and Gym-locomotion are not. For each domain, we consider different classes of baselines for providing comprehensive evaluation. For policy regularization-based methods, the simple method is the canonical behavior cloning (BC) baseline. AWAC [6] and CRR

[8] achieve policy improvement by adding advantage-based weights in the policy loss function. For Q-value constraint methods, CQL [3] and IQL [5] adopt conservative Q-function updates or expectile regression for constraining the policy evaluation process. For sequence modeling approaches, we consider the Decision Transformer (DT) [32] baseline. For diffusion policies, the diffusion Q-learning (DIFF-QL) [15] baseline first represents the policy as a diffusion model, and couples the behavior cloning and policy improvement using WR. Based on DIFF-QL, the efficient diffusion policy (EDP) [10] method approximately constructs actions from corrupted ones for realizing efficient training. CRR+EDP and IQL+EDP respectively adopt CRR and IQL based on EDP for policy improvement. CRR+EDP focuses on advantage-based weight regression, while IQL+EDP uses Q-based weight regression. The SfBC [25] baseline decouples the learned policy into a diffusion behavior model and an action evaluation model, without a policy improvement process.

**Experimental Details.** In our experiments, consistent with the EDP framework, we utilize a critic function network architecture comprising a three-layer MLP, employing the Mish activation function [33]. This architecture is uniformly applied across all tasks. To obtain a more accurate estimate of the Q-value from offline data, the critic function is updated through the IQL approach using expectile regression. The noise prediction network  $\epsilon_{\theta}(\mathbf{a}_t^k, k; s_t)$  of the diffusion policy initially employs sinusoidal embedding [34] to encode timestep  $k$ , subsequently concatenating it with the noisy action  $\mathbf{a}_t^k$  and the conditional state  $s_t$ . Similar to EDP, the policy is trained for 2000 epochs on the Gym-locomotion domain and 1000 epochs on the other domains. Every epoch is made up of 1000 policy updates with a batch size of 256. The third-order version of DPM-Solver [35] is used to perform the denoising process of the diffusion policy with 15 steps. For preferred-action automatic generation, we found that greedy strategy sampling performed outstandingly in most tasks, so we used it. The number of sampled actions is 10, i.e.,  $N = 10$ . Throughout our paper, the results are reported by averaging 3 random seeds. In addition, all the hyperparameters are listed in the Appendix E.

**Evaluation Metrics.** We evaluate the proposed PAO-DP method using two metrics: Online Model Selection (OMS) and Running Average at Training (RAT) [10]. OMS, introduced by Diffusion-QL [15], selects the best-performing model during training, indicating the algorithm’s potential. In contrast, RAT [10] calculates the running average of evaluation performance over ten consecutive checkpoints and reports the final score, providing a more stable and realistic assessment of an algorithm’s performance throughout training. Besides, our paper uses the average normalized score of D4RL to evaluate different methods.

## 4.2 Evaluation Results

We compare our proposed PAO-DP method with the baseline methods across four task domains, with the results detailed in Table 1. The domain-specific analyses are as follows:

**Results for Kitchen Domain:** The Kitchen domain presents a challenging long-term task requiring the agent to accomplish a series of sequential subtasks to reach a goal state configuration. This domain is characterized by sparse rewards and the complexity of achieving the final goal through intermediate steps, making long-term value optimization crucial. The proposed PAO-DP method significantly outperforms the baselines in the Kitchen domain across all three datasets: *Complete*, *Partial*, and *Mixed*. In the *Complete* task, our method achieves an impressive score of 87.2, which is notably higher than the next-best performance of 75.5 by IQL+EDP using WR. The average performance in the Kitchen domain shows PAO-DP at 67.5, demonstrating a substantial improvement over all other methods. These results underscore the effectiveness of PAO-DP in optimizing long-term value in environments with sparse rewards and complex sequential tasks. By integrating policy improvement using preference optimization with diffusion policies, PAO-DP significantly enhances the agent’s performance in this challenging domain, outperforming diffusion policies that incorporate weighted regression.

**Results for AntMaze Domain:** PAO-DP demonstrates superior performance in the AntMaze domain, which is characterized by sparse rewards and challenging sub-optimal trajectory tasks. The average performance across the AntMaze domain for PAO-DP is 79.7, significantly higher than all other baselines. Although CQL marginally surpasses PAO-DP in the *Diverse* task for AntMaze-*umaze*, scoring 84.0 compared to PAO-DP’s 83.7, PAO-DP consistently excels in other settings. The robustness of PAO-DP is particularly evident in the AntMaze-*medium* and AntMaze-*large* tasks, where other methods, such as BC, AWAC, and DT methods, struggle to perform effectively.

Table 1: Average normalized score of the baselines and PAO-OP evaluated using the RAT metric.

Dataset	Environment	BC	AWAC	CQL	IQL	DT	CRR+EDP	IQL+EDP	PAO-DP (Ours)
Complete	Kitchen	33.8	39.3	43.8	62.5	–	73.9	75.5	<b>87.2</b> $\pm$ 1.05
Partial	Kitchen	33.8	36.6	49.8	46.3	–	40.0	46.3	<b>53.3</b> $\pm$ 0.48
Mixed	Kitchen	47.5	22.0	51.0	51.0	–	46.1	56.5	<b>62.2</b> $\pm$ 2.83
<b>Average (FrankaKitchen)</b>		38.4	32.6	48.2	53.3	–	53.3	59.4	<b>67.5</b> $\pm$ 14.45
Dataset	Environment	BC	AWAC	CQL	IQL	DT	CRR+EDP	IQL+EDP	PAO-DP (Ours)
Default	AntMaze-umaze	54.6	56.7	74.0	87.5	59.2	95.9	94.2	<b>97.3</b> $\pm$ 1.69
Diverse	AntMaze-umaze	45.6	49.3	<b>84.0</b>	62.2	53.0	15.9	79.0	<b>83.7</b> $\pm$ 1.69
Play	AntMaze-medium	0.0	0.0	61.2	71.2	0.0	33.5	81.8	<b>85.3</b> $\pm$ 0.47
Diverse	AntMaze-medium	0.0	0.7	53.7	70.0	0.0	32.7	82.3	<b>83.0</b> $\pm$ 2.16
Play	AntMaze-large	0.0	0.0	15.8	39.6	0.0	26.0	42.3	<b>58.7</b> $\pm$ 1.25
Diverse	AntMaze-large	0.0	1.0	14.9	47.5	0.0	58.5	60.6	<b>68.7</b> $\pm$ 0.94
<b>Average (AntMaze)</b>		16.7	18.0	50.6	63.0	18.7	43.8	73.4	<b>79.7</b> $\pm$ 12.10
Dataset	Environment	BC	AWAC	CQL	IQL	DT	CRR+EDP	IQL+EDP	PAO-DP (Ours)
human	pen	25.8	15.6	37.5	71.5	–	70.2	72.7	<b>77.6</b> $\pm$ 0.92
cloned	pen	38.3	24.7	39.2	37.3	–	54.2	70.0	<b>83.6</b> $\pm$ 1.75
<b>Average (Adroit)</b>		32.1	20.2	38.4	54.4	–	62.1	71.3	<b>80.6</b> $\pm$ 3.31
Dataset	Environment	BC	AWAC	CQL	IQL	DT	CRR+EDP	IQL+EDP	PAO-DP (Ours)
Med-Expert	HalfCheetah	55.2	42.8	<b>91.6</b>	86.7	86.8	85.6	86.7	91.0 $\pm$ 0.48
Med-Expert	Hopper	52.5	55.8	105.4	91.5	<b>107.6</b>	92.9	99.6	101.1 $\pm$ 1.01
Med-Expert	Walker	107.5	74.5	108.8	109.6	108.1	<b>110.1</b>	109.0	109.3 $\pm$ 0.05
Medium	HalfCheetah	42.6	43.5	44.0	47.4	42.6	<b>49.2</b>	48.1	47.0 $\pm$ 0.28
Medium	Hopper	52.9	57.0	58.5	66.3	67.6	<b>78.7</b>	63.1	57.4 $\pm$ 0.96
Medium	Walker	75.3	72.4	72.5	78.3	74.0	82.5	<b>85.4</b>	82.3 $\pm$ 1.33
Med-Replay	HalfCheetah	36.6	40.5	<b>45.5</b>	44.2	36.6	43.5	43.8	43.8 $\pm$ 0.04
Med-Replay	Hopper	18.1	37.2	95.0	94.7	82.7	99.0	<b>99.1</b>	90.6 $\pm$ 0.69
Med-Replay	Walker	26.0	27.0	77.2	73.9	66.6	63.3	<b>84.0</b>	83.9 $\pm$ 0.39
<b>Average (Locomotion)</b>		51.9	50.1	77.6	77.0	74.7	78.3	<b>79.9</b>	78.5 $\pm$ 22.23

**Results for Adroit Domain:** The Adroit domain presents unique challenges due to its datasets being primarily collected through human behavior, resulting in a narrow state-action region in the offline data. In the Adroit domain, PAO-DP once again demonstrates its effectiveness. For the *human* dataset in the Adroit-*pen* environment, PAO-DP achieves a score of 77.6, surpassing IQL+EDP’s 72.7 and CRR+EDP’s 70.2. The average performance across the Adroit domain for PAO-DP is 80.6, highlighting its superior capability compared to other methods. These results demonstrate that PAO-DP can maintain high performance within the narrow operational bounds defined by the offline data. The ability of PAO-DP to maintain expected behaviors while improving performance through preference optimization underscores its advantage in constrained environments over the use of weighted regression for policy improvement.

**Results for Locomotion Domain:** The Locomotion domain contains many standard tasks with relatively smooth reward functions. Although PAO-DP does not always achieve the highest scores in this domain, its performance remains competitive and reliable. For the *Med-Expert* dataset in HalfCheetah, PAO-DP scores 91.0, just shy of CQL’s 91.6. In the *Med-Replay* dataset, PAO-DP also performs well, particularly in *Walker* with a score of 83.9, second only to IQL+EDP. The average performance in the Locomotion domain for PAO-DP is 78.5, showcasing its consistent effectiveness across various standard tasks. While the Locomotion domain’s smooth reward functions contrast with the sparse rewards found in domains like Kitchen, PAO-DP’s ability to perform well across these diverse environments underscores its robustness and adaptability. This versatility highlights PAO-DP’s effectiveness in handling a wide range of task complexities.

**Results for Peak Performance Evaluation:** To evaluate the peak performance potential of PAO-DP across different tasks, we conduct experiments using the OMS metric. As illustrated in Table 2, our method demonstrates competitive performance compared to other methods. In the *FrankaKitchen* and *AntMaze* domains, PAO-DP surpasses all baselines, achieving average scores of 80.6 and 96.7,

Table 2: Performance of the baselines and our method evaluated using the OMS metric.

Dataset	DIFF-QL	SfBC	CRR+EDP	IQL+EDP	PAO-DP (Ours)
Average (FrankaKitchen)	69.0	57.1	70.6	79.2	80.6 ± 13.79
Average (AntMaze)	69.6	74.2	76.7	89.2	96.7 ± 4.71
Average (Adroit)	65.1	–	116.9	134.3	121.6 ± 3.06
Average (Locomotion)	88.0	75.6	87.3	84.7	84.1 ± 23.40

respectively. This highlights its robustness in handling sparse rewards and complex trajectory tasks, showcasing its ability to optimize long-term value in challenging environments. For the Adroit domain, PAO-DP scores 121.6, performing competitively against IQL+EDP (134.3) and CRR+EDP (116.9). The relatively smooth reward functions in the Locomotion domain contrast with the sparse rewards found in other domains, potentially diminishing PAO-DP’s relative advantage. Despite this, PAO-DP’s performance remains competitive, underscoring its versatility and robustness across diverse environments.

### 4.3 Ablation Studies

**Comparative Analysis of Diffusion Policy Methods:** As illustrated in Figure 1-(a), the ablation study on the *Kitchen-complete* task underscores the effectiveness of the main component (i.e., preference optimization for policy improvement) of PAO-DP in comparison to other diffusion policy methods. PAO-DP significantly outperforms the DP method, which relies solely on policy cloning using a diffusion model, without any policy improvement. This highlights the benefits of policy improvement using preference optimization. Furthermore, PAO-DP demonstrates superior performance over IQL+EDP and CRR+EDP, both of which employ weighted regression for policy improvement. The sensitivity of WR to Q-value inaccuracies, coupled with constrained optimization using only sample actions within the fixed dataset, limits its efficacy. In contrast, PAO-DP’s strategy of leveraging high-quality preferred actions and incorporating anti-noise preference optimization ensures more stable and robust training, leading to consistently better results in the later training.

**Analysis of Preferred-Action Sampling Strategies:** Figure 1-(b) shows the ablation study on the *Kitchen-complete* task, comparing PAO-DP with different sampling strategies in preferred-action generation. PAO-DP-Max, PAO-DP-Min, and PAO-DP-mean respectively use the action with the highest, lowest, and middle weight  $\exp(\eta Q_\phi(s, a))$  as the preferred action. PAO-DP-Max consistently achieves the best performance, compared with PAO-DP-Min and PAO-DP-Mean, which highlights the advantage of prioritizing actions with the highest weights. This study demonstrates that leveraging the important sampling technique for action selection leads to superior and more stable performance throughout training. More analysis results are shown in the Appendix D.

**Effect of Anti-Noise Optimization** Figure 1-(c) illustrates the ablation study on the *AntMaze-large-play* task, examining the effectiveness of different values of  $\lambda$  in our policy anti-noise preference optimization. As  $\lambda$  increases from 0.0 to 0.4, we observe that the performance improves consistently throughout the training steps. The results demonstrate that incorporating a moderate level of noise helps stabilize the training process and enhances policy improvement, especially in low-quality datasets. More analysis results are shown in the Appendix D.

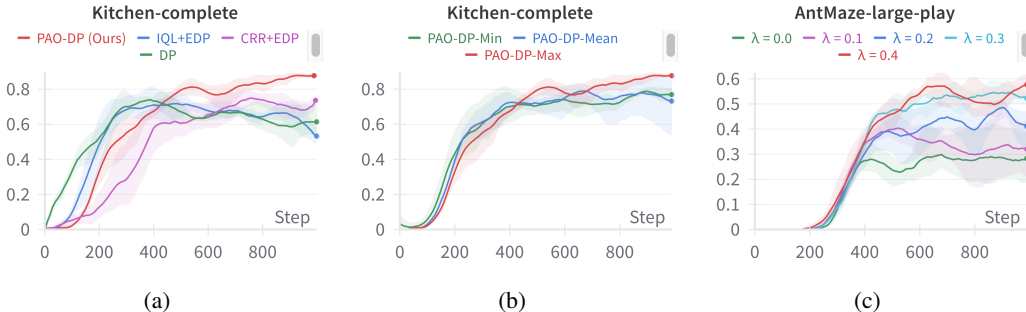


Figure 1: RAT curves of the ablation methods on representative tasks. The ordinate is the average normalized score.



#### 4.4 Sensitivity Analysis to $\xi$

Figure 2 illustrates the sensitivity analysis to the hyperparameter  $\xi$  on the *Kitchen-complete* task for PAO-DP, IQL+EDP, and CRR+EDP. The hyperparameter  $\xi$  can reflect the effect of the policy improvement part in the entire training. In Figure 2-(a), PAO-DP demonstrates robust performance across different  $\xi$  values, showing minimal sensitivity to changes in  $\xi$ . Conversely, Figures 2-(b) and 2-(c) illustrate that both IQL+EDP and CRR+EDP exhibit significant instability to  $\xi$ , which indicates that the weighted regression for policy improvement has training instability. The analysis further verifies the robustness and effectiveness of the policy improvement part using the preference optimization of our method.

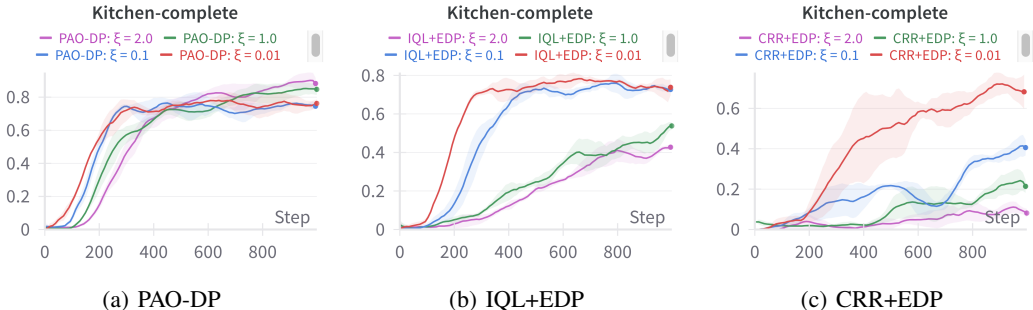


Figure 2: RAT curves for different methods with different  $\xi$  on the *Kitchen-complete* task. The ordinate is the average normalized score.

### 5 Related Work

**Policy Regularization and Conservative Estimation.** Policy regularization and pessimistic conservative estimation are important approaches to addressing offline RL issues [36–39]. Policy regularization methods introduce regularization terms during the policy improvement process. For instance, the earliest proposed BCQ [2] directly improves a policy perturbation model based on the behavior model of CVAE [40]. Based on this, some works such as BEAR [41] and TD3+BC [7] incorporate the loss of behavior cloning into the policy improvement process by minimizing Maximum Mean Discrepancy (MMD) or maximizing likelihood estimation. Additionally, BRAC [42] has explored regularization methods in KL divergence, MMD, and Wasserstein duality. On the other hand, some works [43, 44] introduce pessimistic conservative estimation during policy evaluation to mitigate extrapolation errors caused by out-of-distribution actions. For instance, CQL [3] supplements an additional penalty term in Q-values estimation to achieve a non-pointwise lower bound estimation of Q-values. Additionally, some works such as CRR [8] and IQL [5] have achieved promising performance by leveraging advantage actions or within-distribution sampling.

**Diffusion and Transformer in RL.** The powerful sequence modeling capability and multi-modal representation ability of diffusion models and transformers enable them to be widely explored in RL [45–48]. Early proposals such as DT [32] and TT [49] are based on the transformer framework to generate state sequences or action-state sequences maximizing returns from expected trajectory rewards. On the other hand, the multi-modal representation capability of diffusion models enables them to exhibit significant advantages in offline RL tasks with datasets featuring multi-modal distributions [50, 51]. Diffusion-RL [15] is the first exploration of diffusion policies in reinforcement learning policy modeling under multi-modal datasets. To guide policy sampling towards actions with high Q-values, some works [52, 10] construct policies as Q-value-guided conditional generative policies through weighted regression. In addition, some approaches [25, 50] decouple policy learning into behavior learning and action evaluation and introduce in-distribution sampling to avoid extrapolation errors. To incorporate explicit Q-value guidance, some work [15, 53] further subtracts the weighted expectation of Q-values during policy training to guide diffusion policy updates.

### 6 Conclusion

This paper proposes a novel preferred-action-optimized diffusion policy (PAO-DP) for offline RL. PAO-DP utilizes a preference model with preferred actions to improve the diffusion policy, instead of weighted regression. In particular, a conditional diffusion model is used to represent the distribution

of behavior policy. Preferred actions are automatically generated through the critic function based on the diffusion model. Moreover, an anti-noise preference optimization using the preferred actions is designed to improve the policy. To the best of our knowledge, this paper is the first attempt to combine preference optimization and diffusion models for offline RL. Experimental results on the D4RL benchmark demonstrate that PAO-DP has competitive or superior performance compared to other RL methods. Ablation studies and parameter sensitivity analysis further validate the effectiveness of the key components of PAO-DP.

## References

- [1] Sergey Levine, Aviral Kumar, George Tucker, and Justin Fu. Offline reinforcement learning: Tutorial, review, and perspectives on open problems. *arXiv preprint arXiv:2005.01643*, 2020.
- [2] Scott Fujimoto, David Meger, and Doina Precup. Off-policy deep reinforcement learning without exploration. In *International conference on machine learning*, pages 2052–2062. PMLR, 2019.
- [3] Aviral Kumar, Aurick Zhou, George Tucker, and Sergey Levine. Conservative q-learning for offline reinforcement learning. *Advances in Neural Information Processing Systems*, 33: 1179–1191, 2020.
- [4] Tianhe Yu, Aviral Kumar, Rafael Rafailov, Aravind Rajeswaran, Sergey Levine, and Chelsea Finn. Combo: Conservative offline model-based policy optimization. *Advances in neural information processing systems*, 34:28954–28967, 2021.
- [5] Ilya Kostrikov, Ashvin Nair, and Sergey Levine. Offline reinforcement learning with implicit q-learning. In *International Conference on Learning Representations*, 2021.
- [6] Ashvin Nair, Abhishek Gupta, Murtaza Dalal, and Sergey Levine. Awac: Accelerating online reinforcement learning with offline datasets. *arXiv preprint arXiv:2006.09359*, 2020.
- [7] Scott Fujimoto and Shixiang Shane Gu. A minimalist approach to offline reinforcement learning. *Advances in neural information processing systems*, 34:20132–20145, 2021.
- [8] Ziyu Wang, Alexander Novikov, Konrad Zolna, Josh S Merel, Jost Tobias Springenberg, Scott E Reed, Bobak Shahriari, Noah Siegel, Caglar Gulcehre, Nicolas Heess, et al. Critic regularized regression. *Advances in Neural Information Processing Systems*, 33:7768–7778, 2020.
- [9] Xiao Ma, Bingyi Kang, Zhongwen Xu, Min Lin, and Shuicheng Yan. Mutual information regularized offline reinforcement learning. *Advances in Neural Information Processing Systems*, 36, 2024.
- [10] Bingyi Kang, Xiao Ma, Chao Du, Tianyu Pang, and Shuicheng Yan. Efficient diffusion policies for offline reinforcement learning. *Advances in Neural Information Processing Systems*, 36, 2024.
- [11] Jonathan Ho, Ajay Jain, and Pieter Abbeel. Denoising diffusion probabilistic models. *Advances in neural information processing systems*, 33:6840–6851, 2020.
- [12] Jiaming Song, Chenlin Meng, and Stefano Ermon. Denoising diffusion implicit models. *arXiv preprint arXiv:2010.02502*, 2020.
- [13] Prafulla Dhariwal and Alexander Nichol. Diffusion models beat gans on image synthesis. *Advances in neural information processing systems*, 34:8780–8794, 2021.
- [14] Robin Rombach, Andreas Blattmann, Dominik Lorenz, Patrick Esser, and Björn Ommer. High-resolution image synthesis with latent diffusion models. In *Proceedings of the IEEE/CVF conference on computer vision and pattern recognition*, pages 10684–10695, 2022.
- [15] Zhendong Wang, Jonathan J Hunt, and Mingyuan Zhou. Diffusion policies as an expressive policy class for offline reinforcement learning. In *The Eleventh International Conference on Learning Representations*, 2022.

- [16] Yecheng Ma, Dinesh Jayaraman, and Osbert Bastani. Conservative offline distributional reinforcement learning. *Advances in neural information processing systems*, 34:19235–19247, 2021.
- [17] Long Ouyang, Jeffrey Wu, Xu Jiang, Diogo Almeida, Carroll Wainwright, Pamela Mishkin, Chong Zhang, Sandhini Agarwal, Katarina Slama, Alex Ray, et al. Training language models to follow instructions with human feedback. *Advances in neural information processing systems*, 35:27730–27744, 2022.
- [18] Rafael Rafailov, Archit Sharma, Eric Mitchell, Christopher D Manning, Stefano Ermon, and Chelsea Finn. Direct preference optimization: Your language model is secretly a reward model. *Advances in Neural Information Processing Systems*, 36, 2024.
- [19] Ralph Allan Bradley and Milton E Terry. Rank analysis of incomplete block designs: I. the method of paired comparisons. *Biometrika*, 39(3/4):324–345, 1952.
- [20] Justin Fu, Aviral Kumar, Ofir Nachum, George Tucker, and Sergey Levine. D4rl: Datasets for deep data-driven reinforcement learning. *arXiv preprint arXiv:2004.07219*, 2020.
- [21] Martin L Puterman. *Markov decision processes: discrete stochastic dynamic programming*. John Wiley & Sons, 2014.
- [22] Xinyue Chen, Zijian Zhou, Zheng Wang, Che Wang, Yanqiu Wu, and Keith Ross. Bail: Best-action imitation learning for batch deep reinforcement learning. *Advances in Neural Information Processing Systems*, 33:18353–18363, 2020.
- [23] Rishabh Agarwal, Dale Schuurmans, and Mohammad Norouzi. An optimistic perspective on offline reinforcement learning. In *International Conference on Machine Learning*, pages 104–114. PMLR, 2020.
- [24] Xue Bin Peng, Aviral Kumar, Grace Zhang, and Sergey Levine. Advantage-weighted regression: Simple and scalable off-policy reinforcement learning. *arXiv preprint arXiv:1910.00177*, 2019.
- [25] Huayu Chen, Cheng Lu, Chengyang Ying, Hang Su, and Jun Zhu. Offline reinforcement learning via high-fidelity generative behavior modeling. In *The Eleventh International Conference on Learning Representations*, 2022.
- [26] Yang Song and Stefano Ermon. Generative modeling by estimating gradients of the data distribution. *Advances in neural information processing systems*, 32, 2019.
- [27] David M Blei, Alp Kucukelbir, and Jon D McAuliffe. Variational inference: A review for statisticians. *Journal of the American statistical Association*, 112(518):859–877, 2017.
- [28] Joey Hejna and Dorsa Sadigh. Inverse preference learning: Preference-based rl without a reward function. *Advances in Neural Information Processing Systems*, 36, 2024.
- [29] Scott Fujimoto, Herke Hoof, and David Meger. Addressing function approximation error in actor-critic methods. In *International conference on machine learning*, pages 1587–1596. PMLR, 2018.
- [30] Eric Mitchell. A note on dpo with noisy preferences and relationship to ipo. *arxiv*, 2023. URL <https://ericmitchell.ai/cdpo.pdf>.
- [31] Sayak Ray Chowdhury, Anush Kini, and Nagarajan Natarajan. Provably robust dpo: Aligning language models with noisy feedback. *arXiv preprint arXiv:2403.00409*, 2024.
- [32] Lili Chen, Kevin Lu, Aravind Rajeswaran, Kimin Lee, Aditya Grover, Misha Laskin, Pieter Abbeel, Aravind Srinivas, and Igor Mordatch. Decision transformer: Reinforcement learning via sequence modeling. *Advances in neural information processing systems*, 34:15084–15097, 2021.
- [33] Diganta Misra. Mish: A self regularized non-monotonic activation function. *arXiv preprint arXiv:1908.08681*, 2019.

- [34] Ashish Vaswani, Noam Shazeer, Niki Parmar, Jakob Uszkoreit, Llion Jones, Aidan N Gomez, Łukasz Kaiser, and Illia Polosukhin. Attention is all you need. *Advances in neural information processing systems*, 30, 2017.
- [35] Cheng Lu, Yuhao Zhou, Fan Bao, Jianfei Chen, Chongxuan Li, and Jun Zhu. Dpm-solver: A fast ode solver for diffusion probabilistic model sampling in around 10 steps. *Advances in Neural Information Processing Systems*, 35:5775–5787, 2022.
- [36] Gaon An, Seungyong Moon, Jang-Hyun Kim, and Hyun Oh Song. Uncertainty-based offline reinforcement learning with diversified q-ensemble. *Advances in Neural Information Processing Systems*, 34, 2021.
- [37] Wenxuan Zhou, Sujay Bajracharya, and David Held. Plas: Latent action space for offline reinforcement learning. In *Conference on Robot Learning*, 2020.
- [38] Hua Wei, Deheng Ye, Zhao Liu, Hao Wu, Bo Yuan, Qiang Fu, Wei Yang, and Zhenhui Li. Boosting offline reinforcement learning with residual generative modeling. In *International Joint Conference on Artificial Intelligence*, 2021.
- [39] Jiayi Guan, Shangding Gu, Zhijun Li, Jing Hou, Yiqin Yang, Guang Chen, and Changjun Jiang. Uac: Offline reinforcement learning with uncertain action constraint. *IEEE Transactions on Cognitive and Developmental Systems*, 2023.
- [40] Kihyuk Sohn, Honglak Lee, and Xinchen Yan. Learning structured output representation using deep conditional generative models. *Advances in neural information processing systems*, 28, 2015.
- [41] Aviral Kumar, Justin Fu, Matthew Soh, George Tucker, and Sergey Levine. Stabilizing off-policy q-learning via bootstrapping error reduction. *Advances in neural information processing systems*, 32, 2019.
- [42] Yifan Wu, George Tucker, and Ofir Nachum. Behavior regularized offline reinforcement learning. *arXiv preprint arXiv:1911.11361*, 2019.
- [43] Jiayi Guan, Guang Chen, Jiaming Ji, Long Yang, Ao Zhou, Zhijun Li, and changjun jiang. VOCE: Variational optimization with conservative estimation for offline safe reinforcement learning. In *Thirty-seventh Conference on Neural Information Processing Systems*, 2023.
- [44] Jiayi Guan, Li Shen, Ao Zhou, Lusong Li, Han Hu, Xiaodong He, Guang Chen, and Changjun Jiang. POCE: Primal policy optimization with conservative estimation for multi-constraint offline reinforcement learning. In *Conference on Computer Vision and Pattern Recognition*, 2024.
- [45] Wenhao Li, Xiangfeng Wang, Bo Jin, and Hongyuan Zha. Hierarchical diffusion for offline decision making. In *International Conference on Machine Learning*, pages 20035–20064. PMLR, 2023.
- [46] Anurag Ajay, Yilun Du, Abhi Gupta, Joshua B Tenenbaum, Tommi S Jaakkola, and Pulkit Agrawal. Is conditional generative modeling all you need for decision making? In *The Eleventh International Conference on Learning Representations*, 2022.
- [47] Thomas A Berrueta, Allison Pinosky, and Todd D Murphey. Maximum diffusion reinforcement learning. *Nature Machine Intelligence*, pages 1–11, 2024.
- [48] Mengdi Xu, Yikang Shen, Shun Zhang, Yuchen Lu, Ding Zhao, Joshua Tenenbaum, and Chuang Gan. Prompting decision transformer for few-shot policy generalization. In *international conference on machine learning*, pages 24631–24645. PMLR, 2022.
- [49] Michael Janner, Qiyang Li, and Sergey Levine. Offline reinforcement learning as one big sequence modeling problem. *Advances in neural information processing systems*, 34:1273–1286, 2021.
- [50] Cheng Lu, Huayu Chen, Jianfei Chen, Hang Su, Chongxuan Li, and Jun Zhu. Contrastive energy prediction for exact energy-guided diffusion sampling in offline reinforcement learning. In *International Conference on Machine Learning*, pages 22825–22855. PMLR, 2023.

- [51] Philippe Hansen-Estruch, Ilya Kostrikov, Michael Janner, Jakub Grudzien Kuba, and Sergey Levine. Idql: Implicit q-learning as an actor-critic method with diffusion policies. *arXiv preprint arXiv:2304.10573*, 2023.
- [52] Kehua Chen, Xianda Chen, Zihan Yu, Meixin Zhu, and Hai Yang. Equidiff: A conditional equivariant diffusion model for trajectory prediction. In *2023 IEEE 26th International Conference on Intelligent Transportation Systems (ITSC)*, pages 746–751. IEEE, 2023.
- [53] Suzan Ece Ada, Erhan Oztop, and Emre Ugur. Diffusion policies for out-of-distribution generalization in offline reinforcement learning. *IEEE Robotics and Automation Letters*, 2024.

## A The overall design of PAO-DP

To visually present the proposed method, the overall design of PAO-DP is further shown in Fig. 3.

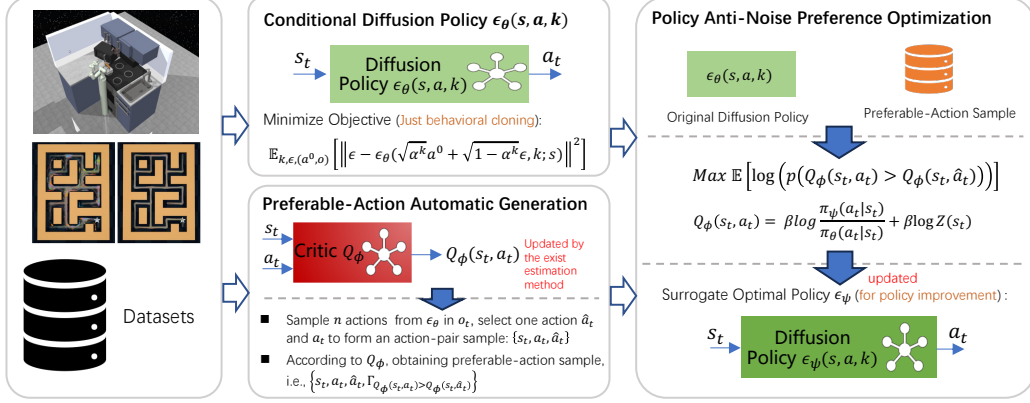


Figure 3: Overall design of the proposed method

## B Mathematical Derivations

### B.1 The Optimal Closed-form Solution of the Regularized Objective in Offline RL

In offline RL, we follow previous works [24, 6, 25] by maximizing the expected Q-value under policy  $\pi(a|s)$  while constraining the distance between policy  $\pi(a|s)$  and the behavior policy  $\pi^b(a|s)$ . Therefore, the objective can be represented as  $J(\pi) = \arg \max_{\pi} \mathbb{E}_s [\sum_a \pi(a|s) Q_\phi(s, a)] - \eta \mathbb{E}_s [D_{KL}(\pi(\cdot|s) || \pi^b(\cdot|s))]$ . Consequently, the optimal closed-form solution for this objective can be expressed as:

$$\pi^*(\cdot|s) = \frac{1}{Z(s)} \pi^b(\cdot|s) \exp \left[ \frac{1}{\eta} Q_\phi(s, a) \right]. \quad (17)$$

**Proof.** We review the objective of offline RL with a regularization term, and expanding the KL divergence term of the regularization yields the following expression:

$$\begin{aligned} J(\pi) &= \arg \max_{\pi} \mathbb{E}_s \left[ \sum_a \pi(a|s) Q_\phi(s, a) \right] - \eta \mathbb{E}_s [D_{KL}(\pi(\cdot|s) || \pi^b(\cdot|s))] \\ &= \arg \max_{\pi} \mathbb{E}_s \left[ \sum_a \pi(a|s) Q_\phi(s, a) \right] - \eta \mathbb{E}_s \left[ \sum_a \pi(\cdot|s) \log \frac{\pi(\cdot|s)}{\pi^b(\cdot|s)} \right] \\ &= \arg \max_{\pi} \mathbb{E}_s \left[ \sum_a \pi(a|s) Q_\phi(s, a) \right] - \eta \mathbb{E}_s \left[ \sum_a \pi(\cdot|s) [\log \pi(\cdot|s) - \log \pi^b(\cdot|s)] \right]. \end{aligned} \quad (18)$$

To derive the closed-form solution for Eq. (18), we differentiate Eq. (18) concerning  $\pi(a|s)$ , resulting in the following expression:

$$\begin{aligned} &\mathbb{E}_s \left[ \sum_a \pi(a|s) Q_\phi(s, a) \right] - \eta \mathbb{E}_s \left[ \sum_a \pi(\cdot|s) [\log \pi(\cdot|s) - \log \pi^b(\cdot|s)] \right]'_{\pi(\cdot|s)} \\ &\stackrel{\{i\}}{=} \mathbb{E}_s Q_\phi(s, a) - \eta \mathbb{E}_s \left[ \log \pi(\cdot|s) - \log \pi^b(\cdot|s) + \sum_a \pi(\cdot|s) \frac{1}{\pi(\cdot|s)} \right] \\ &= \mathbb{E}_s \left[ Q_\phi(s, a) - \eta \log \frac{\pi(\cdot|s)}{\pi^b(\cdot|s)} - \eta \right]. \end{aligned} \quad (19)$$

In practical computations, the KL divergence typically employs the natural logarithm base  $e$ . Consequently, in step  $\{i\}$ ,  $[\log \pi(\cdot|s)]'_{\pi(\cdot|s)} = \pi(\cdot|s)^{-1}$  holds true. To obtain the explicit expression of the

closed-form solution  $\pi^*(\cdot|s)$  for Eq. (18), we set Eq (19) to zero  $\mathbb{E}_{\mathbf{s}} \left[ Q_{\phi}(\mathbf{s}, \mathbf{a}) - \eta \log \frac{\pi(\cdot|\mathbf{s})}{\pi^b(\cdot|\mathbf{s})} - \eta \right] = 0$ , yielding the following expression:

$$\begin{aligned} Q_{\phi}(\mathbf{s}, \mathbf{a}) - \eta \log \frac{\pi^*(\cdot|\mathbf{s})}{\pi^b(\cdot|\mathbf{s})} - \eta = 0 &\iff \log \frac{\pi^*(\cdot|\mathbf{s})}{\pi^b(\cdot|\mathbf{s})} = \eta Q(\mathbf{s}, \mathbf{a}) - 1 \\ \iff \pi^*(\cdot|\mathbf{s}) &= \pi^b(\cdot|\mathbf{s}) \exp\left[\frac{1}{\eta} Q(\mathbf{s}, \mathbf{a}) - 1\right] \\ \iff \pi^*(\cdot|\mathbf{s}) &= \frac{1}{Z(\mathbf{s})} \pi^b(\cdot|\mathbf{s}) \exp\left[\frac{1}{\eta} Q(\mathbf{s}, \mathbf{a})\right] \end{aligned} \quad (20)$$

where  $\pi^*$  is the optimal closed-form solution of Eq. 18, and  $Z(\mathbf{s}) = \exp(1)$  is the partition function.

From Eq. (20), it is evident that there is a direct relationship between the policy  $\pi^*(\mathbf{a}|s)$  and the behavior policy  $\pi^b(\mathbf{a}|s)$ . However, accurately estimating the behavior policy  $\pi^b(\mathbf{a}|s)$  is challenging. Therefore, following previous work[24, 8, 22, 25], we project the policy  $\pi^*(\mathbf{a}|s)$  onto the parameterized policy  $\pi_{\theta}(\mathbf{a}|s)$ . Consequently, the final optimization objective can be expressed as:

$$J(\pi_{\theta}) = \arg \max_{\theta} \mathbb{E}_{(\mathbf{s}, \mathbf{a}) \sim \mathcal{D}} \left[ \frac{1}{Z(\mathbf{s})} \log \pi_{\theta}(\mathbf{a}|\mathbf{s}) \exp\left(\frac{1}{\eta} Q_{\phi}(\mathbf{s}, \mathbf{a})\right) \right]. \quad (21)$$

**Proof.** We utilize the KL divergence to constrain the distance between  $\pi^*$  and  $\pi_{\theta}$ , achieving the projection of  $\pi^*$  onto the parameterized  $\pi_{\theta}$ . The The derivation process can be expressed as follows:

$$\begin{aligned} &\arg \min_{\theta} \mathbb{E}_{\mathbf{s} \sim \mathcal{D}} [D_{KL}(\pi^*(\cdot|\mathbf{s}) || \pi_{\theta}(\cdot|\mathbf{s}))] \\ &= \arg \min_{\theta} \mathbb{E}_{\mathbf{s} \sim \mathcal{D}} \left[ \sum_{\mathbf{a}} \pi^*(\cdot|\mathbf{s}) [\log \pi^*(\cdot|\mathbf{s}) - \log \pi_{\theta}(\cdot|\mathbf{s})] \right] \\ &= \arg \min_{\theta} \mathbb{E}_{\mathbf{s} \sim \mathcal{D}} \mathbb{E}_{\mathbf{a} \sim \pi^*(\cdot|\mathbf{s})} [\log \pi^*(\cdot|\mathbf{s}) - \log \pi_{\theta}(\cdot|\mathbf{s})] \\ &= \arg \min_{\theta} \underbrace{\mathbb{E}_{\mathbf{s} \sim \mathcal{D}} \mathbb{E}_{\mathbf{a} \sim \pi^*(\cdot|\mathbf{s})} \log \pi^*(\cdot|\mathbf{s})}_{\mathcal{C}} - \mathbb{E}_{\mathbf{s} \sim \mathcal{D}} \mathbb{E}_{\mathbf{a} \sim \pi^*(\cdot|\mathbf{s})} \log \pi_{\theta}(\cdot|\mathbf{s}) \\ &\stackrel{\{i\}}{\iff} \arg \min_{\theta} -\mathbb{E}_{\mathbf{s} \sim \mathcal{D}} \mathbb{E}_{\mathbf{a} \sim \pi^*(\cdot|\mathbf{s})} \log \pi_{\theta}(\cdot|\mathbf{s}) \\ &\iff \arg \max_{\theta} \mathbb{E}_{\mathbf{s} \sim \mathcal{D}} \mathbb{E}_{\mathbf{a} \sim \pi^*(\cdot|\mathbf{s})} \log \pi_{\theta}(\cdot|\mathbf{s}) \\ &= \arg \max_{\theta} \mathbb{E}_{\mathbf{s} \sim \mathcal{D}} \left[ \sum_{\mathbf{a}} \pi^*(\cdot|\mathbf{s}) \log \pi_{\theta}(\cdot|\mathbf{s}) \right] \\ &= \arg \max_{\theta} \mathbb{E}_{\mathbf{s} \sim \mathcal{D}} \left[ \sum_{\mathbf{a}} \pi^b(\cdot|\mathbf{s}) \frac{\pi^*(\cdot|\mathbf{s})}{\pi^b(\cdot|\mathbf{s})} \log \pi_{\theta}(\cdot|\mathbf{s}) \right] \\ &= \arg \max_{\theta} \mathbb{E}_{\mathbf{s} \sim \mathcal{D}} \mathbb{E}_{\mathbf{a} \sim \pi^b(\cdot|\mathbf{s})} \left[ \frac{\pi^*(\cdot|\mathbf{s})}{\pi^b(\cdot|\mathbf{s})} \log \pi_{\theta}(\cdot|\mathbf{s}) \right] \\ &\stackrel{\{ii\}}{=} \arg \max_{\theta} \mathbb{E}_{\mathbf{s} \sim \mathcal{D}} \mathbb{E}_{\mathbf{a} \sim \pi^b(\cdot|\mathbf{s})} \left[ \frac{\frac{1}{Z(\mathbf{s})} \pi^b(\cdot|\mathbf{s}) \exp\left[\frac{1}{\eta} Q(\mathbf{s}, \mathbf{a})\right]}{\pi^b(\cdot|\mathbf{s})} \log \pi_{\theta}(\cdot|\mathbf{s}) \right] \\ &= \arg \max_{\theta} \mathbb{E}_{\mathbf{s} \sim \mathcal{D}} \mathbb{E}_{\mathbf{a} \sim \pi^b(\cdot|\mathbf{s})} \left[ \frac{1}{Z(\mathbf{s})} \log \pi_{\theta}(\cdot|\mathbf{s}) \exp\left[\frac{1}{\eta} Q(\mathbf{s}, \mathbf{a})\right] \right] \\ &\stackrel{\{iii\}}{=} \arg \max_{\theta} \mathbb{E}_{\mathbf{s} \sim \mathcal{D}} \mathbb{E}_{\mathbf{a} \sim \mathcal{D}} \left[ \frac{1}{Z(\mathbf{s})} \log \pi_{\theta}(\cdot|\mathbf{s}) \exp\left[\frac{1}{\eta} Q(\mathbf{s}, \mathbf{a})\right] \right] \\ &= \arg \max_{\theta} \mathbb{E}_{(\mathbf{s}, \mathbf{a}) \sim \mathcal{D}} \left[ \frac{1}{Z(\mathbf{s})} \log \pi_{\theta}(\cdot|\mathbf{s}) \exp\left[\frac{1}{\eta} Q(\mathbf{s}, \mathbf{a})\right] \right] \end{aligned} \quad (22)$$

where  $Z(\mathbf{s})$  is the same partition function as in Eq. (20). In step  $\{i\}$ , since  $\mathbb{E}_{\mathbf{s} \sim \mathcal{D}} \mathbb{E}_{\mathbf{a} \sim \pi^*(\cdot|\mathbf{s})} [\log \pi^*(\cdot|\mathbf{s})]$  is a constant concerning the parameter  $\theta$  during the optimization of Eq. (22), it does not affect the maximization objective and can thus be directly ignored. In step  $\{ii\}$ , Eq. (20) is substituted into the current equation. In step  $\{iii\}$ ,  $\pi^b(\mathbf{a}|s)$  is the behavior policy of the dataset  $\mathcal{D}$ , thus  $\pi^b(\mathbf{a}|s) \sim \mathcal{D}$ .

## B.2 Deriving the Preference Optimization Objective of PAO-DP Under the Bradley-Terry Model

In Section 3.3, the popular Bradley-Terry (BT) model [19, 18] is used to model the preference distribution  $p^*$  for actions:

$$p^*(\hat{\mathbf{a}}_t \succ \mathbf{a}_t | \mathbf{s}_t) = \frac{\exp(Q(\mathbf{s}_t, \hat{\mathbf{a}}_t))}{\exp(Q(\mathbf{s}_t, \hat{\mathbf{a}}_t)) + \exp(Q(\mathbf{s}_t, \mathbf{a}_t))}. \quad (23)$$

Given Eq. (23), we can directly derive the preference optimization objective of PAO-DP under the BT preference model. Meanwhile, in Section 3.3, based on Eq. (2), we can express the ground-truth Q-value through its corresponding optimal policy:

$$Q(\mathbf{s}_t, \mathbf{a}_t) = \eta \log \frac{\pi^*(\mathbf{a}_t | \mathbf{s}_t)}{\pi^b(\mathbf{a}_t | \mathbf{s}_t)} + \eta \log Z(\mathbf{s}), \quad (24)$$

Substituting Eq. (24) into Eq. (23) we obtain:

$$\begin{aligned} p^*(\hat{\mathbf{a}}_t \succ \mathbf{a}_t | \mathbf{s}_t) &= \frac{\exp\left(\eta \log \frac{\pi^*(\hat{\mathbf{a}}_t | \mathbf{s}_t)}{\pi^b(\hat{\mathbf{a}}_t | \mathbf{s}_t)} + \eta \log Z(\mathbf{s})\right)}{\exp\left(\eta \log \frac{\pi^*(\hat{\mathbf{a}}_t | \mathbf{s}_t)}{\pi^b(\hat{\mathbf{a}}_t | \mathbf{s}_t)} + \eta \log Z(\mathbf{s})\right) + \exp\left(\eta \log \frac{\pi^*(\mathbf{a}_t | \mathbf{s}_t)}{\pi^b(\mathbf{a}_t | \mathbf{s}_t)} + \eta \log Z(\mathbf{s})\right)} \\ &= \frac{\exp(\eta \log Z(\mathbf{s})) \exp\left(\eta \log \frac{\pi^*(\hat{\mathbf{a}}_t | \mathbf{s}_t)}{\pi^b(\hat{\mathbf{a}}_t | \mathbf{s}_t)}\right)}{\exp(\eta \log Z(\mathbf{s})) \left[ \exp\left(\eta \log \frac{\pi^*(\hat{\mathbf{a}}_t | \mathbf{s}_t)}{\pi^b(\hat{\mathbf{a}}_t | \mathbf{s}_t)}\right) + \exp\left(\eta \log \frac{\pi^*(\mathbf{a}_t | \mathbf{s}_t)}{\pi^b(\mathbf{a}_t | \mathbf{s}_t)}\right) \right]} \\ &= \frac{\exp\left(\eta \log \frac{\pi^*(\hat{\mathbf{a}}_t | \mathbf{s}_t)}{\pi^b(\hat{\mathbf{a}}_t | \mathbf{s}_t)}\right)}{\exp\left(\eta \log \frac{\pi^*(\hat{\mathbf{a}}_t | \mathbf{s}_t)}{\pi^b(\hat{\mathbf{a}}_t | \mathbf{s}_t)}\right) + \exp\left(\eta \log \frac{\pi^*(\mathbf{a}_t | \mathbf{s}_t)}{\pi^b(\mathbf{a}_t | \mathbf{s}_t)}\right)} \\ &= \frac{1}{1 + \exp\left(\eta \log \frac{\pi^*(\mathbf{a}_t | \mathbf{s}_t)}{\pi^b(\mathbf{a}_t | \mathbf{s}_t)} - \eta \log \frac{\pi^*(\hat{\mathbf{a}}_t | \mathbf{s}_t)}{\pi^b(\hat{\mathbf{a}}_t | \mathbf{s}_t)}\right)} \\ &= \sigma\left(\eta \log \frac{\pi^*(\hat{\mathbf{a}}_t | \mathbf{s}_t)}{\pi^b(\hat{\mathbf{a}}_t | \mathbf{s}_t)} - \eta \log \frac{\pi^*(\mathbf{a}_t | \mathbf{s}_t)}{\pi^b(\mathbf{a}_t | \mathbf{s}_t)}\right), \end{aligned} \quad (25)$$

$\sigma$  is the logistic function. The final line represents the per-instance loss in Eq. (15).

## C More Results

Table 3 presents the detailed performance of various baseline methods and our proposed PAO-DP evaluated using the OMS metric across multiple environments. For the *FrankaKitchen* domain, PAO-DP consistently outperforms other methods, particularly excelling in the *Complete* dataset. This indicates PAO-DP’s ability to handle tasks requiring sequential subtask completion. In the *AntiMaze* domain, PAO-DP again demonstrates superior performance, achieving perfect scores in different datasets. This highlights the method’s effectiveness in navigating complex mazes and dealing with sparse rewards. For the *Adroit* domain, although PAO-DP’s average score of 121.6 is slightly lower than IQL+EDP, it remains competitive, showing strong performance in human and cloned tasks. This reflects its capability in high-dimensional robotic manipulation tasks. In the *Locomotion* domain, the performance is more varied. PAO-DP performs well in some tasks but shows a wider range in scores. This variability suggests that while PAO-DP is versatile, its relative advantage may be reduced in environments with smoother reward functions compared to sparse-reward settings. This may be because in sparse-reward environments, preferred actions with significant quality differences can be generated, efficiently promoting preference optimization for policy improvement, but less in smooth-reward environments. Overall, PAO-DP demonstrates robust and competitive performance across diverse and challenging environments, particularly excelling in scenarios with complex trajectories and sparse rewards.

## D More Ablation Analysis

**Analysis of Preferred-Action Sampling Strategies.** Figures 4-(a) and 4-(b) explore scenarios where  $\lambda = 0.0$ , indicating the absence of the anti-noise strategy. In the relatively noise-free *Kitchen-complete* dataset, PAO-DP-Max shows superior performance, suggesting that in datasets with minimal



Table 3: Performance of the baselines and PAO-OP evaluated using the OMS metric.

Dataset	Environment	DIFF-QL	CRR+EDP	IQL+EDP	PAO-DP (Ours)
Complete	Kitchen	84.0	95.8	95.0	100.0 ± 0.00
Partial	Kitchen	60.5	56.7	72.5	70.0 ± 2.04
Mixed	Kitchen	62.5	59.2	70.0	71.8 ± 0.94
Average (FrankaKitchen)		69.0	70.6	79.2	80.6 ± 13.79
Default	AntMaze-umaze	93.6	98.0	98.0	100.0 ± 0.0
Diverse	AntMaze-umaze	66.2	80.0	90.0	100.0 ± 0.0
Play	AntMaze-medium	76.6	82.0	89.0	100.0 ± 0.0
Diverse	AntMaze-medium	78.6	72.0	88.0	100.0 ± 0.0
Play	AntMaze-large	46.4	57.0	52.0	90.0 ± 0.0
Diverse	AntMaze-large	56.6	71.0	68.0	90.0 ± 0.0
Average (AntMaze)		69.6	76.7	89.2	96.7 ± 4.71
human	pen	72.8	127.8	130.3	124.1 ± 1.59
cloned	pen	57.3	106.0	138.2	119.2 ± 2.05
Average (Adroit)		65.1	116.9	134.3	121.6 ± 3.06
Medium-Expert	HalfCheetah	96.8	93.5	80.9	92.4 ± 0.27
Medium-Expert	Hopper	111.1	109.4	95.7	111.1 ± 0.97
Medium-Expert	Walker	110.1	112.3	111.5	110.6 ± 0.49
Medium	HalfCheetah	51.1	50.2	48.7	47.4 ± 0.25
Medium	Hopper	90.5	95.0	97.3	71.4 ± 1.27
Medium	Walker	87.0	85.8	88.7	88.0 ± 0.31
Medium-Replay	HalfCheetah	47.8	47.8	45.5	44.5 ± 0.10
Medium-Replay	Hopper	101.3	101.7	100.9	100.8 ± 0.49
Medium-Replay	Walker	95.5	89.8	93.4	90.9 ± 0.67
Average (Locomotion)		88.0	87.3	84.7	84.1 ± 23.40

noise, the highest sampling weight is reliable and effective because high-quality actions may be close to the distribution of optimal actions. Conversely, in the more complex and randomization *AntMaze-large-play* dataset, PAO-DP-Max performs less reliably, highlighting that in challenging settings, the highest sampling weight may lead to sub-optimal policy updates. Figures 4-(b) and 4-(c) further illustrate the impact of introducing the anti-noise mechanism by varying  $\lambda$ . With  $\lambda = 0.0$ , PAO-DP-Max’s performance is significantly lower compared to PAO-DP-Mean and PAO-DP-Min, indicating unreliability in relatively noisy datasets. However, increasing  $\lambda$  to 0.4 shows a recovery in PAO-DP-Max’s performance, aligning it closely with optimal results observed in PAO-DP-Mean and PAO-DP-Min. This recovery underscores the effectiveness of the anti-noise strategy in mitigating the adverse effects of noise, enhancing robustness, and improving policy reliability. This analysis highlights the critical role of preferred-action sampling strategies for policy improvement and the need for rational selection of the sampling strategies based on the anti-noise parameter  $\lambda$ .

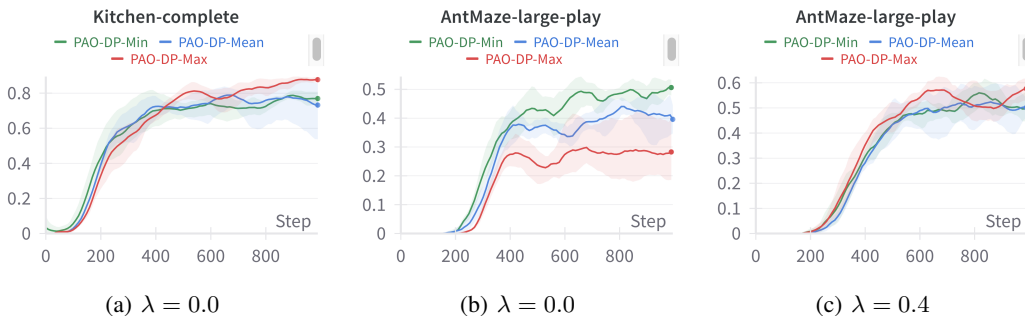


Figure 4: Performance of PAO-DP variants in *Kitchen-complete* and *AntMaze-large-play* environments, comparing different sampling strategies with  $\lambda = 0.0$  and  $\lambda = 0.4$ .

**The Impact of  $\lambda$  on Different Tasks.** Figure 5-(a) illustrates that in the relatively noise-free *Kitchen-complete* dataset, PAO-DP-Max with different  $\lambda$  values yields similar performance outcomes, indicating the minimal impact of the anti-noise strategy. This suggests that in low-noise datasets,

policy performance remains robust across various  $\lambda$  settings, with the highest sampling weight (PAO-DP-Max) consistently achieving excellent results. In contrast, Figure 5-(b) reveals significant performance variations in the *AntMaze-large-play* environment as  $\lambda$  increases. With  $\lambda = 0.0$ , performance is notably lower, especially for PAO-DP-Max (See Figure 4-(b)), highlighting the challenges posed by the complex and noisy nature of this environment. As  $\lambda$  increases, performance improves, particularly for  $\lambda = 0.4$ , where PAO-DP-Max aligns closely with PAO-DP-Mean and PAO-DP-Min (See Figure 4-(c)). This indicates that the proposed anti-noise mechanism effectively mitigates noise, enhancing policy reliability and robustness in challenging noisy, complex settings.

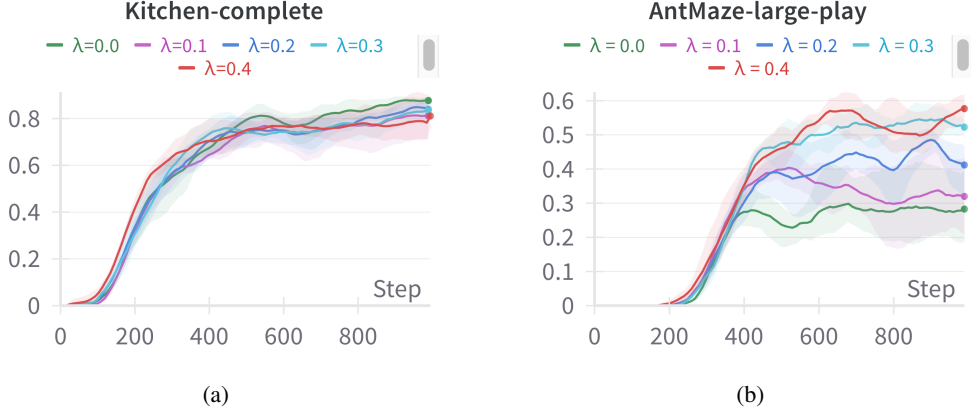


Figure 5: Impact of varying  $\lambda$  values on PAO-DP performance in Kitchen-complete and AntMaze-large-play environments.

## E Hyperparameters

The detailed hyperparameters of the proposed method are presented in Table 4.

Table 4: Hyperparameters of PAO-DP.

Dataset	Environment	Learning rate	Epochs	Batch size	$\eta$	$\lambda$	$\xi$
Complete	Kitchen	3e-4	1000	256	0.1	0.0	1.0
Partial	Kitchen	3e-4	1000	256	0.1	0.2	1.0
Mixed	Kitchen	3e-4	1000	256	0.1	0.2	1.0
Default	AntMaze-umaze	3e-4	1000	256	0.1	0.2	1.0
Diverse	AntMaze-umaze	3e-4	1000	256	0.1	0.2	1.0
Play	AntMaze-medium	3e-4	1000	256	0.1	0.1	1.0
Diverse	AntMaze-medium	2e-4	1000	256	0.1	0.5	1.0
Play	AntMaze-large	1e-4	1000	256	0.1	0.4	1.0
Diverse	AntMaze-large	1e-4	1000	256	0.1	0.4	1.0
human	pen	1e-4	1000	256	0.1	0.4	1.0
cloned	pen	5e-5	1000	256	0.1	0.2	1.0
Medium-Expert	HalfCheetah	3e-4	2000	256	0.1	0.2	1.0
Medium-Expert	Hopper	3e-4	2000	256	0.1	0.2	1.0
Medium-Expert	Walker	3e-4	2000	256	0.1	0.2	1.0
Medium	HalfCheetah	3e-4	2000	256	0.1	0.2	1.0
Medium	Hopper	3e-4	2000	256	0.1	0.2	1.0
Medium	Walker	3e-4	2000	256	0.1	0.1	1.0
Medium-Replay	HalfCheetah	3e-4	2000	256	0.1	0.1	1.0
Medium-Replay	Hopper	3e-4	2000	256	0.1	0.1	1.0
Medium-Replay	Walker	3e-4	2000	256	0.1	0.4	1.0

## **F Limitations and Future Work**

The effectiveness of the proposed PAO-DP hinges on accurate Q-value estimation to select preferred actions. However, offline RL continues to grapple with the out-of-distribution problem, where discrepancies between evaluation and training data may lead to Q-value estimation errors. These inaccuracies propagate throughout the learning process, resulting in suboptimal policy performance. Additionally, the accuracy of Q-values is impacted by the quality and complexity of datasets, further challenging the robustness of the policy.

Future research could enhance PAO-DP by incorporating trajectory-based preference optimization. We directly generate preferred trajectory data for preference optimization, instead of preferred action data using Q-values. This avoids the OOD problem using Q-values. We can compare two trajectories based on success or time to generate preferred trajectory data. This approach is expected to improve policy robustness and generalization, especially in complex environments. In addition, developing methods to encode and utilize trajectory information, possibly using advanced sequence modeling techniques, holds promise for more stable and strong offline RL.